geosciences

MDPI

Article

New Discovery of Middle Jurassic Dinosaur Tracks in Chaya County, Eastern Tibet, China

Gao Zhu [1], Li Yangui [1,*], Yao Huazhou [2], Liu Yilei [1], Xing Lida [3], Ye Qiang [4], Huang Jinghou [5], Wang Jianhua [1] and Chen Lin [6,*]

[1] College of Mining Engineering, Guizhou University of Engineering Science, Bijie 551700, China; gaozhu520@126.com (G.Z.); liu_yilei@163.com (L.Y.); wjhcumt@163.com (W.J.)
[2] Wuhan Center, China Geological Survey (Geosciences Innovation Center of Central South China), Wuhan 430205, China; ycxc2009@126.com
[3] State Key Laboratory of Geomicrobiology and Environmental Changes, School of Earth Sciences and Resources, Frontiers Science Center for Deep-time Digital Earth, China University of Geosciences, Beijing 100083, China; xinglida@gmail.com
[4] Regional Geological Survey Team, Tibet Autonomous Region Geological and Mineral Exploration Bureau, Lhasa 851400, China; 18189911872@163.com
[5] Longkou Municipal Bureau of Natural Resources and Planning, Longkou 265701, China; huangjinghou@163.com
[6] School of Urban Construction and Safety Engineering, Hubei University of Education, Wuhan 430205, China
* Correspondence: liyangui1992@gues.edu.cn (L.Y.); chenlin676@163.com (C.L.); Tel.: +86-183-2714-8800 (L.Y.); +86-182-0271-2940 (C.L.)

Abstract

The Changdu Basin in eastern Tibet was an important habitat for Jurassic dinosaur faunas, yet reports of dinosaur remains are scarce. Research on the composition of dinosaur assemblages, palaeoenvironments, and palaeobiogeography remains insufficient. This paper reports a dinosaur tracksite from the Middle Jurassic Dabuka Formation in Duolongwa Village, Chaya County, and discusses ichnomorphology, the trackmakers, their gait and speed, and sedimentary facies. Two tracklayers are observed. Theropod tracks from the DLW1 theropod tracklayer are assigned to Eubrontidae ichnogen. et ichnosp. indet. (Morphotype-1). The trackmakers had hip heights of 0.98–1.71 m and body lengths of 2.59–4.48 m and primarily moved at a walking gait. *Gasosaurus constructus* is the most probable trackmaker. Sauropod tracks from the DLW2 sauropod tracklayer are assigned to *Brontopodus* isp. (Morphotype-2). The trackmakers had an estimated hip height of 2.96 m and a body length of 10.94 m. They were likely juveniles belonging to the *Shunosaurus–Mamenchisaurus* fauna. Sedimentological analyses indicate that the Duolongwa tracksite was a general fluvial depositional system characterized by channel-related and overbank deposits. The discovery of the Duolongwa tracksite demonstrates close links between the Middle Jurassic dinosaur fauna of eastern Tibet and contemporaneous dinosaur faunas of the Sichuan–Yunnan areas, providing new evidence for faunal exchange among dinosaur assemblages across Southwest China.

Keywords: Qinghai–Tibet Plateau; sauropod; theropod; Dabuka Formation

Academic Editor: Michele Morsilli

Received: 18 September 2026
Revised: 10 November 2026
Accepted: 11 November 2026
Published: 19 November 2026

Copyright: © 2026 by the authors. Licensee MDPI, Basel, Switzerland. This article is an open access article distributed under the terms and conditions of the Creative Commons Attribution (CC BY) license.

1. Introduction

The terrestrial red-bed basins of southwestern China are important regions for global Jurassic dinosaur research. The Mesozoic strata of Sichuan and Yunnan provinces have yielded abundant dinosaur remains and tracks, forming a complete and continuous evolutionary succession of dinosaur faunas. This succession includes the Early Jurassic *Lufengosaurus* [1] and *Zizhongosaurus* faunas [2], the Middle Jurassic *Chuanjiesaurus* [3] and *Shunosaurus–Omeisaurus* faunas [4,5], and the Late Jurassic *Mamenchisaurus* fauna [6], representing characteristic dinosaur faunas of East Asia. In the Jurassic deposits, theropod and sauropod tracks are abundant, providing a solid basis for reconstructing regional dinosaur evolution and paleobiogeographic exchange [1,7–9]. The Changdu Basin in eastern Tibet is adjacent to the two major fossil-rich areas of Sichuan and Yunnan. Mesozoic continental clastic rocks are widely exposed in the basin, covering approximately 11,000 km^2 [10–12]. These deposits provide favorable sedimentary conditions for preserving dinosaur fossils. However, fieldwork constraints associated with the high-altitude, cold climate, and complex terrain of the Qinghai–Tibet Plateau have limited studies of dinosaurs from eastern Tibet. Published dinosaur remains and tracks are scarce and scattered, in stark contrast to the more extensive research conducted in Sichuan and Yunnan.

Chao et al. [13,14] were the first to report Jurassic dinosaur remains in the Changdu area. However, the Early and Middle Jurassic species established from these specimens were later regarded as nomina nuda because the original materials were lost and the taxonomic assignments lacked adequate supporting evidence [15–17]. In addition, *Monkonosaurus lawulacus* [18] from the Upper Jurassic–Lower Cretaceous [19] is represented only by sacrals [20] and lacks sufficient diagnostic features. Therefore, it has been regarded as a nomen dubium [21]. In recent years, researchers have discovered fragmentary sauropod and theropod remains in Chaya County. These fossils are considered potentially related to the contemporaneous dinosaur fauna of southwestern China. Dinosaur tracks from the Middle Jurassic of the Changdu Basin are the most abundant. Xing et al. [17,22,23] reported at least eight sauropod tracksites dominated by *Brontopodus* and one tracksite with a *Deltapodus* trackway. Yao et al. [24] and Li et al. [25–27] focused on theropod footprints and suggested that this assemblage can be assigned to the *Grallator–Eubrontes* plexus. Chen et al. [28] reported the world's smallest sauropod footprint, *Parabrontopodus* isp., as well as a theropod trackway attributable to Eubrontidae. Weise et al. [29] also reported a newly discovered theropod trackway, although it remains unidentified at the genus and species levels and has not been studied in detail. In addition, Early Cretaceous sauropod, ornithopod, and theropod footprints [30], Late Cretaceous ornithopod and sauropod footprints [31], and bird tracks [32] have been reported. Recent studies indicate that eastern Tibet was an important Jurassic dinosaur habitat, yet its record remains poorly documented. Tracksites are poorly documented, and dinosaur remains are rare. Although dinosaur tracks are more abundant, they have not been thoroughly studied. Limited comparisons with coeval dinosaur faunas from adjacent regions limit our understanding of this assemblage. The Duolongwa tracksite described in this study contains one sauropod tracklayer and one newly identified theropod tracklayer from eastern Tibet. Here, we describe the tracksite, provide an ichnological analysis of the tracks, discuss the paleogeographic distribution of tracks in eastern Asia, and infer the trackmakers, their gait, and the depositional paleoenvironment.

2. Geological Background

The Changdu Basin lies within the eastern Tethys orogenic domain, sandwiched between the Jinshajiang tectonic belt and the Lancangjiang tectonic belt. In the Late Triassic,

as the Jinshajiang and Lancangjiang Oceans closed sequentially, the Changdu region transitioned from marine to continental conditions during the Early Jurassic. The paleogeographic isolation between it and the central Yunnan Basin of Yunnan Province, as well as the Sichuan Basin of Sichuan Province, was removed. This coastal inland basin became a key habitat for the evolution and survival of Jurassic dinosaurs in East Asia [30,31,33].

The Duolongwa tracksite is located south of the Changdu Basin (Figure 1A), approximately 4 km southeast of Duolongwa Village, Chaya County, Changdu City (Figure 1B; coordinates: 97°54′35″ E, 30°31′16″ N). The Duolongwa Section is exposed along Provincial Road S203 and comprises the Middle Jurassic Dabuka Formation (Figure 1C,D), which is subdivided into four units. Unit-1 and Unit-2 are dominated by purple-red, very thick-bedded massive medium- to fine-grained sandstone, locally interbedded with purple-red thin- to very thin-bedded argillaceous siltstone or silty mudstone (Figure 1E). Unit-3 consists of gray-green, thick-bedded massive medium- to fine-grained sandstone, with occasional interbeds of purple-red or gray-green thin-bedded muddy siltstone or argillaceous siltstone, and rare thin conglomerate layers (Figure 1F). Unit-4 is composed of purple-red, thick- to very thick-bedded medium- to fine-grained sandstone, locally interbedded with purple-red thin- to medium-bedded argillaceous siltstone (Figure 1G).

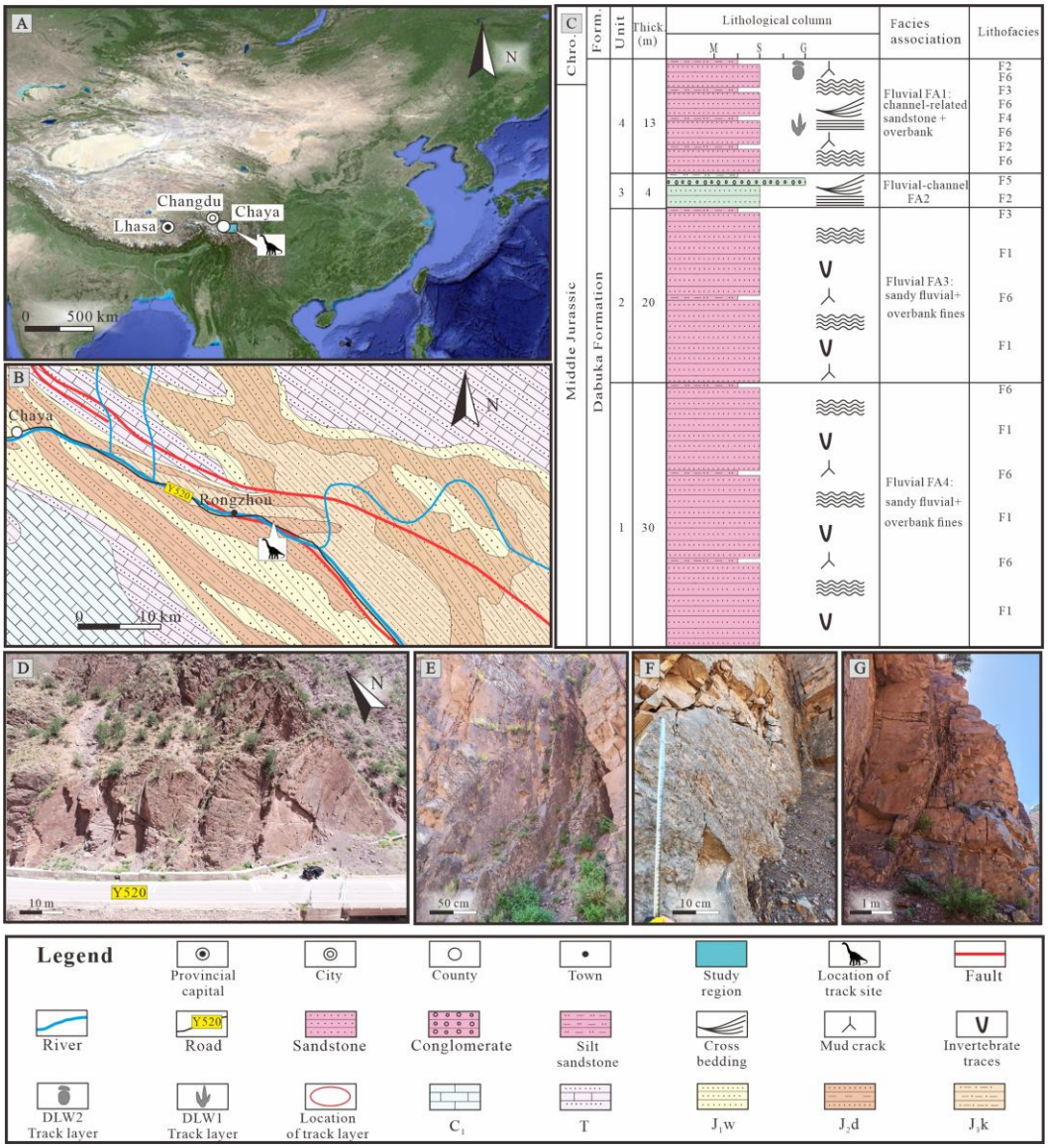


Figure 1. (**A**), Geographic location of the study area; (**B**), simplified geological map of the study area (after Wang et al.) [34]; (**C**), lithological column of the Duolongwa Section; (**D**), photograph of the

https://doi.org/10.3390/geosciences16110482

Duolongwa Section; (**E**), photograph of Unit-1 and Unit-2; (**F**), photograph of Unit-3; (**G**), photograph of Unit-4 (Chro. = Chronostratigraphy; Form. = Formation; M = mudstone; S = sandstone; G = conglomerate; DLW1 = DLW1 theropod tracklayer; DLW2 = DLW2 sauropod tracklayer; C_1 = Lower Carboniferous; T = Triassic; J_1w = Lower Jurassic Wangbu Formation; J_2d = Middle Jurassic Dabuka Formation; J_3k = Upper Jurassic Kenzuoga Formation).

According to He et al. [35], the sporopollen taxa *Classopollis* and *Psophosphaer* reported in the Dabuka Formation are characteristic taxa of the Early and Middle Jurassic. In addition, the Dabuka Formation has yielded several common Middle Jurassic freshwater bivalves from western Yunnan, including *Lamprotula (Eolamprotula) cremeri*, *Pseudocardinia kweichouensis*, *Pse. angulate*, *Pse.* cf. *khadjakalanensis*, *Unio yunnanensis*, *Psilunio ovalis*, *Psi. lufengensis*, *Psi. thailandicus*, *Psi.* cf. *Yuanmouensis*, *Cuneopsis johannisboehmi*, and *C. sichuanensis*. Therefore, the geological age of the Dabuka Formation is generally considered to be Middle Jurassic [14,36].

3. Materials and Methods

The Duolongwa Section was exposed by road-cut slope excavation. The tracklayers dip at approximately 80°, and two tracklayers are present (Figure 1C,D). The tracks were discovered following erosion of the overlying muddy siltstone, and except track 2-2, all tracks are preserved in situ as concave epireliefs. The DLW1 theropod tracklayer covers approximately 14 m^2 and is located 8.3 m above the base of Unit-4; 12 theropod tracks are visible (Figure 2).

The DLW2 sauropod tracklayer covers approximately 13 m^2 and is located 1.5 m below the top of Unit-4; two sauropod tracks are visible (Figure 3).

After numbering all tracks, approximately 40 photographs were taken of each track from different directions. These photographs were imported into Agisoft Metashape Professional (1.6.3 × 64) to generate a 3D height image. Interpretive outline drawings were then drawn in CorelDRAW 2017.

Following Zhen et al. [37], we created a schematic diagram for measuring track data. According to Thulborn's [38] criteria, the measured parameters include pedal track length (FL) and pedal track width (FW). For theropod tracks, additional measurements include the interdigit divarication angles between digits II and III (α), the interdigit divarication angles between digits III and IV (β), and the interdigit divarication angles between digits II and IV ($\alpha + \beta$). Trackway measurements for theropods include pace length (PL), stride length (SL), pedal track pace angulation (ANG), and rotation of pedal track relative to the mid-line of trackway (γ; "-" means the imprint is rotated inward; otherwise it is rotated outward). According to the methods proposed by Olsen et al. [39] and Lockley et al. [40], we calculated the mesaxony of digit III (a/b) and the projection ratio (X/Y) of the theropod tracks. Following Xing et al. [41] and Henderson et al. [42], the hip height (H) and body length (L) of the theropod trackmakers were estimated using the equations H = 4.9FL (Equation (1)) and L = 2.63H (Equation (2)), respectively. The body size of sauropod trackmakers was estimated using the equations proposed by Alexander et al. [43] and Farlow et al. [44], where H = 5.3FL (Equation (3)) and L = 3.7H (Equation (4)).

This study also discusses the gait and speed (V) of the trackmakers. Thulborn et al. [38] modified the empirical formula of Alexander et al. [43] and suggested that when SL/H ≤ 2 (Equation (5)), the trackmaker was walking slowly, and $V = 0.25\, g^{0.5}\, SL^{1.67}\, H^{-1.17}$ (Equation (6)). When 2 < SL/H < 2.9 (Equation (7)), the trackmaker was moving at a trotting gait, and when SL/H ≥ 2.9 (Equation (8)), the trackmaker was running quickly, with $V = [gH(SL/1.8H)^{2.56}]^{0.5}$ (Equation (9)). Here, g = 9.8 m/s^2.

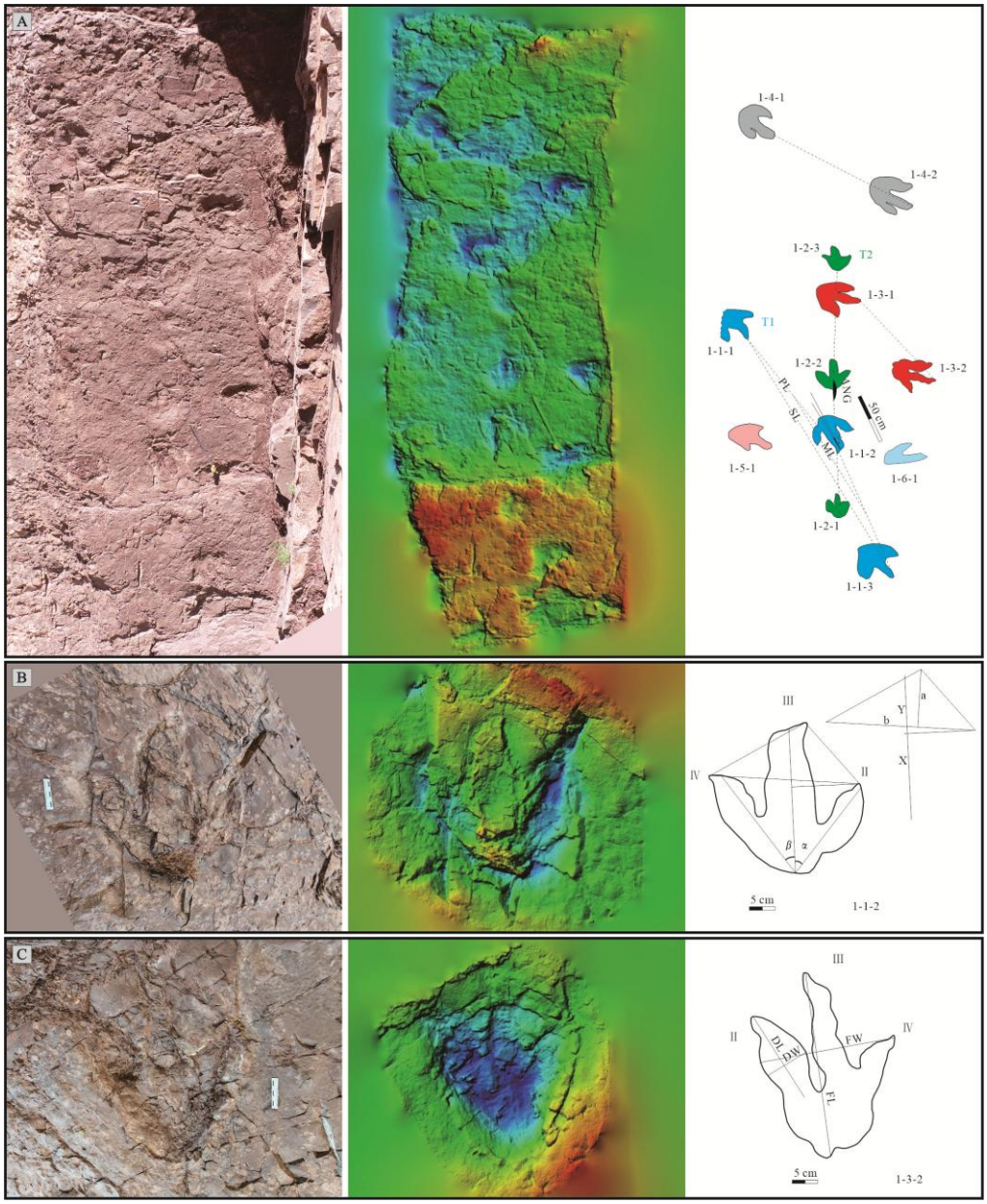


Figure 2. Photograph, 3D height images (warm colors = high areas, cool colors = low areas), and interpretive outline drawings of Morphotype-1 in DLW1 theropod tracklayer. (**A**), DLW1 theropod tracklayer; (**B**), 1-1-2; (**C**), 1-3-2. (T1 = T1 trackway; T2 = T2 trackway; ML = mid-line of trackway; PL = pace length; SL = stride length; ANG = pedal track pace angulation; γ = rotation of pedal track relative to the mid-line of trackway; II = digit II; III = digit III; IV = digit IV; a/b = mesaxony of digit III; X/Y = projection ratio; α = interdigit divarication angles between digits II and III; β = interdigit divarication angles between digits III and IV; FL = pedal track length; FW = pedal track width; DL = digit length; DW = digit width).

In addition to the ichnological investigation, we conducted a sedimentological analysis of the exposed Dabuka Formation succession at the Duolongwa Section. We documented lithological features, including rock type, bed thickness, and bedding geometry, as well as sedimentary structures such as trough cross-bedding, parallel bedding, climbing-ripple cross-lamination, ripple marks, mud cracks, and erosional surfaces. Lithofacies were identified on the basis of their diagnostic lithological and sedimentological characteristics. We then examined their vertical distribution, stacking patterns, and associations to assess changes in depositional processes and sedimentary environments. Particular at-

tention was given to the relationships between sandstone bodies and fine-grained interbeds and to evidence of channel erosion, current-driven sediment transport, low-energy deposition, and periodic subaerial exposure. Finally, the lithofacies were grouped into facies associations based on their sedimentological characteristics and stratigraphic relationships, providing a basis for interpreting the fluvial depositional environments represented by the track-bearing succession.

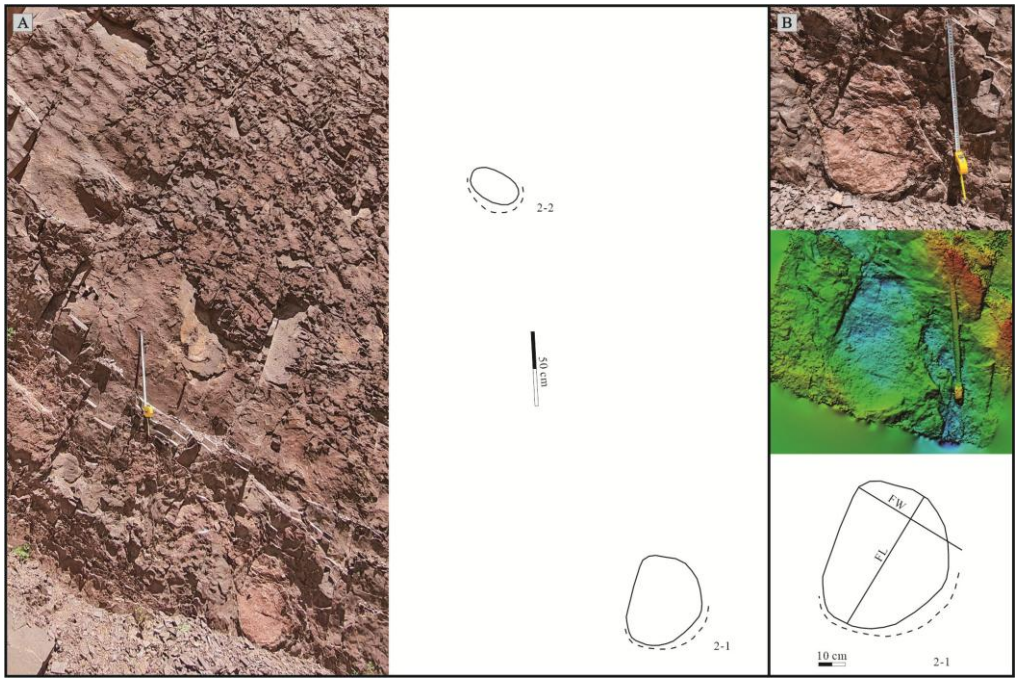


Figure 3. (**A**), Photograph of the DLW2 sauropod tracklayer and an interpretive outline drawing showing the track distribution; (**B**), photograph, 3D height image (warm colors = high areas, cool colors = low areas), and interpretative outline drawings of 2-1 (FL = pedal track length; FW = pedal track width).

4. Morphological Paleontology

4.1. Eubrontidae igen. et isp. indet. Morphotype-1

Description. A total of 11 pedal tracks are preserved in situ as concave epireliefs on the DLW1 theropod tracklayer. They were left by a bipedal, tridactyl, digitigrade trackmaker; no manual or tail tracks are observed (Figure 2A). T1 Trackway (T1) consists of three tracks (right pedal track 1-1-1, left pedal track 1-1-2, and right pedal track 1-1-3). SL1-1-1 is 206.1 cm, PL1-1-1 is 107.5 cm, PL1-1-2 is 101.0 cm, ANG1-1-2 is 165°, and γ1-1-2 is -2°. Tracks 1-1-1 and 1-1-3 are poorly preserved, and the digit impressions are difficult to discern. Track 1-1-2 (Figure 2B) is the best preserved. It has an FL of 29.6 cm and an FW of 29.8 cm, with α (40°) > β (36°). Digit III is the longest (DLIII = 19.2 cm, DWIII = 9.1 cm), followed by digit II (DLII = 11.2 cm, DWII = 6.1 cm) and digit IV (DLIV = 11.1 cm, DWIV = 6.9 cm). The digits are robust, but the phalangeal pads are poorly preserved. The distal phalangeal pads of digit III are rounded, and claw marks are visible at the distal ends of the digits, with the claw mark on digit III being the largest. A rounded metatarsophalangeal pad is present at the posterior end of the track, with a distinct concavity between it and digit II. T2 Trackway (T2) consists of three tracks (right pedal track 1-2-1, left pedal track 1-2-2, and right pedal track 1-2-3). SL1-2-1 is 182.6 cm, the mean PL is 91.4 cm, and ANG1-2-2 and γ1-2-2 are 175° and -3°, respectively. All three tracks are poorly preserved, and the digit impressions are difficult to discern; therefore, only FL and FW were measured, with mean values of 20.1 cm and 21.2 cm, respectively. Left pedal track 1-3-1 and

right pedal track 1-3-2 are two successive tracks (PL1-3-1 = 80.3 cm), but 1-3-1 is poorly preserved, with indistinct phalangeal pads and digit impressions. Track 1-3-2 (Figure 2C) is relatively well preserved, with FL and FW of 36.2 cm and 27.1 cm, respectively, and α and β of 24° and 27°. Digit III is the longest (DLIII = 24.1 cm, DWIII = 6.3 cm), with three well-preserved rounded phalangeal pads. Digit II is relatively robust (DLII = 19.2 cm, DWII = 9.0 cm), and digit IV shows a distal rounded phalangeal pad (DLIV = 10.1 cm, DWIV = 5.2 cm). Sharp claw marks are visible at the distal ends of the digits. A distinctly protruding, small metatarsophalangeal pad is present at the posterior end of the track. Tracks 1-4-1 and 1-4-2 are successive (PL1-4-1 = 114.3 cm), and both are poorly preserved; their mean FL and FW are 32.9 cm and 26.4 cm, respectively. Tracks 1-5-1 and 1-6-1 are also poorly preserved. Track 1-5-1 is infilled with purplish-red silty mudstone, with FL and FW of 33.2 cm and 21.3 cm, respectively, whereas 1-6-1 cannot be measured accurately (Table 1).

Remarks. Based on their ichnomorphological features, these theropod tracks can be divided into three types. The type represented by T2 is medium-sized theropod tracks, with FL ranging from 18.2 to 22.1 cm. Their FLs are slightly smaller than the FW, with a mean FL/FW ratio of 0.96, and the phalangeal pads are relatively robust. Because T2 is poorly preserved, the digit impressions are indistinct, and the phalangeal pads, metatarso-phalangeal pads, and claw traces are unclear. Only 1-2-1 and 1-2-2 provide rough estimates of $\alpha + \beta$, X/Y, and a/b values (Table 1); therefore, its ichnotaxonomic assignment remains uncertain.

The type represented by T1 shows some ichnomorphological features of the theropod ichnogenus *Corpulentapus*, first reported by Li et al. [45] from the Lower Cretaceous of Zhucheng, Shandong Province. According to Li et al. [45], *Corpulentapus* is characterized as a bipedal, digitigrade, tridactyl track with robust phalangeal pads, subequal track length and width (FL = 9.5–28.5 cm), broad-digit imprints, and a lily-shaped ichnomorphology. These ichnomorphological features are broadly comparable to those of the tracks of T1 (Figure 2B). However, compared with *Corpulentapus* described by Li et al. [45], the tracks of T1 have a weak mesaxony of digit III and a larger projection ratio. For example, the X/Y values calculated in this study for the holotype of *Corpulentapus* (track no. 214.174) and the 1-1-2 track of T1 are 2.33 and 1.40, respectively, whereas their a/b ratios are 0.32 and 0.39, respectively. Therefore, T1 is more consistent with the ichnofamily Eubrontidae. According to Lull [46], Eubrontidae make large, bipedal, tridactyl tracks with FL generally exceeding 25 cm. The tracks show broad digits and sharply pointed or blunt claw marks, and there is no trace of the tail or manus. The ichnofamily includes six ichnogenera: *Asianopodus* (Matsukawa et al. [47]), *Changpeipus* (Young [48]), *Chapus* (Li Jianjun et al. [49]), *Eubrontes* (Hitchcock et al. [50]), *Hunanpus* (Zeng Xiangyuan [51]), and *Lufengopus* (Lü et al. [52]). These ichnogenera are characterized by distinctly rounded phalangeal pads. *Asianopodus* differs from T1 in having a clear boundary between the metatarso-phalangeal pads and the digital impressions (Matsukawa et al. [47]). *Changpeipus* differs in exhibiting a distinctly rhomboid ichnomorphology (Young [48]). *Chapus* differs by its relatively large digit III claw mark (Li et al. [49]). *Hunanpus* differs by the presence of distal metatarso-phalangeal pads (Zeng [51]), and *Lufengopus* differs by its broad, rounded heel region (Lü et al. [52]). T1, with its well-defined phalangeal pads, broad digit imprints, and blunt claw traces, is most consistent with *Eubrontes*. However, the digits of T1 are more robust than those of typical *Eubrontes*, possibly reflecting a higher moisture content in the substrate at the time of track formation, although not sufficiently high to cause lateral collapse of the sediment due to gravity. A similar preservational condition was reported by Li et al. [53] for *Eubrontes glenrosensis* from the Jurassic of Wulatezhongqi, Neimenggu Province, which likewise shows notably robust digit impressions.

The types represented by 1-3-1 and 1-3-2 are poorly preserved in the metatarso-phalangeal pads, and their digit imprints are indistinct. Nevertheless, they retain some ichnomorphological features of *Eubrontes*, such as sharply pointed claw marks and broad, rounded phalangeal pads. Compared with T1, they have larger FL values than FW values and relatively slender digit imprints. This difference may reflect higher substrate moisture content during T1 formation, leading to deeper foot penetration, more robust impressions, and a larger FW.

T2 cannot be confidently interpreted as any ichnogenus. Although T1, 1-3-1, and 1-3-2 show some ichnomorphological features of *Eubrontes*, their poor preservation precludes a direct assignment to *Eubrontes*. Accordingly, they are here assigned to Eubrontidae igen. et isp. indet.

4.2. Brontopodus isp. (Indeterminate Species), Morphotype-2

Description. Two tracks are preserved in situ on the DLW2 sauropod tracklayer (Figure 3A). Track 2-1 (Figure 3B) is a concave epirelief track. It is elliptical in outline and filled with purplish-red fine sandstone. An expulsion rim is visible. Its FL and FW are 55.8 cm and 45.5 cm, respectively. The digit impressions are indistinct, making it impossible to determine whether it represents a left or right pedal track. Track 2-2 is a convex relief. It is elliptical in outline, with indistinct digit impressions, and it is difficult to distinguish whether it is a manus or pedal track. Only FL and FW were measured for this track (Table 1).

Remarks. The Jurassic sauropod ichnogenera from eastern Asia include *Liujianpus* [54], *Parabrontopodus* [55], and *Brontopodus* [56]. *Brontopodus* is readily distinguished from *Liujianpus* and *Parabrontopodus* by its wide-gauge trackway, whereas the latter two typically exhibit narrow-gauge trackways [54,55]. Reports of Middle Jurassic sauropod tracks from East Asia remain scarce and are concentrated in southwestern Yunnan and eastern Tibet, China.

Xing et al. [57] described a sauropod right pedal track in the Middle Jurassic Chuanjie Formation in Lufeng County, Yunnan Province. It is elliptical, 71.5 cm long, and 54.5 cm wide. They noted indistinct digit impressions, incomplete metatarso-phalangeal pads, and a rounded heel region. Because the trackway information is unclear, they tentatively assigned it to *Brontopodus*. Similarly, Xing et al. [58] reported large sauropod tracks from the nearby Hemenkou area of Shuangbai County, Yunnan Province. These tracks are characterized by elliptical pedal tracks, elliptical to reniform manus tracks, and medium- to wide-gauge trackways. They were assigned to *Brontopodus*.

A newly discovered and important Middle Jurassic sauropod track-bearing region was reported in eastern Tibet. Xing et al. [17] first reported *Brontopodus* from Morong Village, Karuo District, Changdu, where the manus and pedal tracks are elliptical, and the trackway is wide. Later, Xing et al. [22] documented three additional sauropod tracksites in Karuo District, Changdu. According to their description, these specimens were grouped into large, medium, and small types, but their ichnomorphological features are consistent with those from the Morong tracksite. Therefore, they were also assigned to *Brontopodus*. More recently, Xing et al. [23] reported five tracksites in Chaya County. The Duolongwa Tracksite I appears to correspond to the DLW2 sauropod tracklayer investigated in this study. However, during our re-examination, the tracklayer had been damaged, and the tracks illustrated here as 2-1 and 2-2 represent newly exposed specimens. According to the original description, the manus and pedal tracks at Duolongwa Tracksite I are both elliptical; the pedal tracks have lengths of 32.4 cm to 71.5 cm, and the trackway is wide. We therefore follow the interpretation of Xing et al. [23] and tentatively assign Morphotype-2 to *Brontopodus* isp.

Table 1. Measurement data of dinosaur tracks at the Duolongwa tracksite (in centimeters and degrees).

Type	Number	FL	FW	FL/FW	DL-II	DW-II	DL-III	DW-III	DL-IV	DW-IV	α	β	α + β	X/Y	a/b	PL	SL	ANG	γ
M-1	1-1-1	28.2	29.0	0.97	—	—	—	—	—	—	—	—	—	—	—	107.5	206.1	—	—
	1-1-2	29.6	29.8	0.99	11.2	6.1	19.2	9.1	11.1	6.9	40	36	76	1.40	0.39	101.0	—	165	-2
	1-1-3	33.7	33.0	1.02	—	—	—	—	—	—	30	35	65	1.19	0.39	—	—	—	—
	Mean	30.5	30.6	1.00	11.2	6.1	19.2	9.1	11.1	6.9	35	36	71	1.30	0.39	104.3	206.1	165	-2
	1-2-1	18.2	16.9	1.08	—	—	—	—	—	—	31	32	63	1.30	0.32	94.7	182.6	—	—
	1-2-2	22.1	25.2	0.88	9.5	4.3	13.3	6.1	10.1	7.1	38	41	79	1.59	0.32	88.1	—	175	-3
	1-2-3	19.9	21.4	0.93	—	—	—	—	—	—	—	—	—	—	—	—	—	—	—
	Mean	20.1	21.2	0.96	9.5	4.3	13.3	6.1	10.1	7.1	35	37	71	1.45	0.32	91.4	182.6	175	-3
	1-3-1	33.3	25.3	1.32	12.2	9.0	19.6	6.7	12.0	7.8	30	20	50	1.73	0.37	80.3	—	—	—
	1-3-2	36.2	27.1	1.34	19.2	9.0	24.1	6.3	10.1	5.2	24	27	51	1.17	0.36	—	—	—	—
	Mean	34.8	26.2	1.33	15.7	9	21.9	6.5	11.1	6.5	27	24	51	1.45	0.37	80.3	—	—	—
	1-4-1	30.9	25.7	1.20	—	—	—	—	—	—	—	—	—	—	—	114.3	—	—	—
	1-4-2	34.9	27.0	1.29	15.3	8.9	20	6.4	11.3	6.2	26	20	46	2.52	0.35	—	—	—	—
	Mean	32.9	26.4	1.25	15.3	8.9	20	6.4	11.3	6.2	26	20	46	2.52	0.35	—	—	—	—
	1-5-1	33.2	21.3	1.56	—	—	—	—	—	—	—	—	—	—	—	—	—	—	—
	1-6-1	—	—	—	—	—	—	—	—	—	—	—	—	—	—	—	—	—	—
M-2	2-1	55.8	45.5	1.23	—	—	—	—	—	—	—	—	—	—	—	—	—	—	—
	2-2	31.2	18.3	1.70	—	—	—	—	—	—	—	—	—	—	—	—	—	—	—

Note: M-1 = Morphotype-1; M-2 = Morphotype-2; FL = pedal track length; FW = pedal track width; DL = digit length; DW = digit width; II = digit II; III = digit III; IV = digit IV; α = interdigit divarication angles between digits II and III; β = interdigit divarication angles between digits II and III; X/Y = projection ratio; a/b = mesaxony of digit III; PL = pace length; SL = stride length; ANG = pedal track pace angulation; γ = rotation of pedal track relative to the mid-line of trackway ("-" means the imprint is rotated inward; otherwise it is rotated outward).

5. Discussion

5.1. Trackmaker and Gait

5.1.1. Morphotype-1

Based on Equations (1) and (2), the T1 trackmaker is estimated to have had an H of 1.49 m and an L of 3.93 m. Its mean PL and SL are 104.3 cm and 206.1 cm, respectively. The results from Equations 5 and 6 indicate that the trackmaker moved at a slow walking speed (SL/H ≈ 1.38 < 2), with an estimated V of 1.64 m/s. The pedal tracks are slightly rotated inward relative to the midline of the trackway ($\gamma = -2°$), and the ANG is 165°.

The T2 trackmaker is estimated to have had an H of 0.98 m and an L of 2.59 m. Calculations based on Equations 5 and 6 suggest it moved with a slow walking gait (SL/H ≈ 1.85 < 2), with an estimated V of 2.18 m/s, substantially faster than the T1 trackmaker. Similarly to T1, the pes impressions are slightly rotated inward relative to the mid-line of trackway ($\gamma = -3°$); however, the ANG is 175°, which is considerably larger than that of T1, likely reflecting the higher speed of the T2 trackmaker.

Morphotype 1 exhibits several ichnomorphological features consistent with *Eubrontes*, but its classification remains uncertain. Most previous studies have supported a theropod affinity for *Eubrontes* trackmakers[57,59,60]. Although *Eubrontes* tracks have been widely reported in China, their trackmakers have rarely been discussed in detail [61]. Xing et al. [61] proposed, based on dinosaur remains, that the trackmaker of *Eubrontes zigongensis* was *Sinosaurus triassicus* [62], an averostran. However, the tetradactyl footprints of *E. zigongensis* are distinct from other *Eubrontes* specimens, including Morphotype-1 described in this study [33]. More recently, An et al. [15] reported a pair of pubic bones and associated limb remains of a small theropod from Chayu County and suggested a possible affinity with *Shidaisaurus jinae* or *Monolophosaurus*. However, Li et al. [27] argued that the specimen is substantially smaller and suggested that the most likely trackmaker of the Middle Jurassic *Eubrontes* from eastern Tibet is *Gasosaurus constructus*, which was discovered in the adjacent Sichuan Basin and originally described by Dong and Tang (1984) [63]. It had an estimated L of 3.5–4 m. Based on Equations (1) and (2), the estimated L and H of the Morphotype-1 trackmaker are 2.56–4.67 m and 0.98–1.77 m, respectively, values that broadly overlap with the inferred size range of *G. constructus*. Among theropods currently known from southwestern China, *G. constructus* remains the only taxon whose body size is consistent with the Morphotype-1 trackmaker. Although the assignment cannot be confirmed unequivocally based on the evidence, we tentatively follow Li et al. [27] in considering *Gasosaurus constructus* the most likely trackmaker of Morphotype-1.

5.1.2. Morphotype-2

Based on the FL of 2-1, the trackmaker is estimated to have had an H of 2.96 m and an L of 10.94 m, according to Equations (3) and (4). This inferred L is generally smaller than that of the common Middle Jurassic sauropods from southwestern China, including *Shunosaurus* [64] (a maximum L of 12 m), *Omeisaurus* [65] (a maximum L of 20 m), and *Mamenchisaurus* [66] (a maximum L of 26 m).

We follow the view of Xing et al. [14] and tentatively assign Morphotype-2 to *Brontopodus*. Although the Middle Jurassic *Cetiosauridae* and *Brachiosauridae* remains from eastern Tibet reported by Chao [14] have been lost and are now regarded as nomina nuda, An et al. [15,67] noted that these specimens may have some affinity with sauropods from the Sichuan and Yunnan provinces. Xing et al. [22] suggested that the trackmakers of Early to Middle Jurassic *Brontopodus* in southwestern China may be taxa associated with the *Shunosaurus–Mamenchisaurus* fauna, whereas Late Jurassic *Brontopodus* trackmakers are more likely to be Titanosauriformes. Given the discovery of *Brontopodus* in the Middle

Jurassic Chaya Group of eastern Tibet, together with the ichnomorphological similarity between Morphotype-2 and previously described sauropod tracks from eastern Tibet, we follow Xing et al. [23] in interpreting the trackmaker of Morphotype-2 as a member of the *Shunosaurus–Mamenchisaurus* fauna. In addition, subadult *Shunosaurus* individuals from the Sichuan Basin reported by Zhang et al. [68] and Peng et al. [69], with an L of approximately 6 m provide an osteological reference for this inference, suggesting that the Morphotype-2 trackmaker may have been a juvenile or subadult of the *Shunosaurus–Mamenchisaurus* fauna.

5.2. Sedimentological and Paleoenvironmental Analysis

Lithofacies analysis was based on lithology, grain size, sedimentary structures, bed geometry, and the vertical relationships between sandstone and fine-grained deposits. Six lithofacies (F1–F6) were identified in the Duolongwa Section (Table 2). Their associations and vertical organization were then assessed to interpret the depositional processes and environments of the Dabuka Formation. Here, lithofacies refers to a sediment body identified by its characteristic sedimentological features, whereas facies association refers to a group of genetically related lithofacies interpreted on the basis of their spatial and stratigraphic relationships.

Unit-1 and Unit-2 consist predominantly of purplish-red, thick- to very thick-bedded, medium- to fine-grained sandstone, locally interbedded with thin- to very thin-bedded argillaceous siltstone and silty mudstone. The sandstone is commonly massive or lacks clearly discernible internal stratification at outcrop scale (F1); climbing-ripple cross-lamination occurs locally (F3; Figure 4A). Combined-flow ripple marks, characterized by sinuous, asymmetrical crests, are abundant on some sandstone bedding surfaces (Figure 4B). These ripple marks suggest interaction between unidirectional currents and oscillatory flows, whereas climbing-ripple cross-lamination records ripple migration accompanied by sediment accumulation [27,70–72]. Neither structure alone is diagnostic of point-bar deposition. The thin-bedded argillaceous siltstone and silty mudstone interbeds are poorly laminated and locally exhibit polygonal mud cracks (F6). Their fine grain size indicates deposition predominantly from suspension under low-energy conditions, while the mud cracks record subsequent subaerial exposure and desiccation. The association of sandstone facies F1 and F3 with fine-grained facies F6 therefore indicates alternation between sandy fluvial deposition and low-energy fine-grained sedimentation in areas subject to intermittent flooding and exposure. The fine-grained deposits are consistent with overbank sedimentation, potentially in floodplain depressions [70,73]. However, the available observations do not identify a specific floodplain subenvironment or establish that all sandstone beds represent point bars. Accordingly, Unit-1 and Unit-2 are interpreted as a fluvial depositional interval comprising sandy deposits and fine-grained overbank deposits. Further subdivision into individual facies successions requires assessment of bed boundaries, vertical grain-size trends, and sedimentary architecture in the measured section.

Unit-3 is composed predominantly of grayish-green, thick-bedded, massive, medium-grained sandstone with parallel bedding (F4), trough cross-bedding (F2), and locally lenticular bed geometries. Thin conglomerate beds (F5) are intercalated with the sandstone. The conglomerate clasts are moderately to well sorted, subrounded to rounded, and preferentially oriented. An erosional scour surface occurs at the base of one conglomerate bed (Figure 4C). The association of conglomeratic facies F5 with cross-bedded sandstone facies F2 and parallel-bedded sandstone facies F4 indicates erosion, sediment transport, and deposition by unidirectional currents in a fluvial channel [74–76]. The basal scour surface records channel-bed erosion, while the conglomerate represents dep-

osition of relatively coarse material under energetic flow conditions, potentially as a channel lag. The associated sandstone records continued sand transport and deposition during channel activity. Where a systematic upward-fining succession is present, it may record waning flow energy and progressive channel filling [74–76]. Taken together, these facies support interpretation of Unit-3 as a fluvial-channel facies association. However, the observed structures do not, on their own, distinguish a meandering river from a braided or other fluvial channel system. Such a distinction requires evidence from channel architecture, lateral accretion, and the organization of successive channel deposits.



Figure 4. (**A**), Photograph of alternations of purplish-red medium- to thick-bedded medium- to fine-grained sandstone and medium- to thin-bedded silty mudstone in Unit-1 and Unit-2, climbing-ripple cross-lamination and wedge-shaped pinch-outs in the sandstone beds; (**B**), asymmetrical ripples developed on the sandstone bedding surface of Unit-1; (**C**), grayish-green thick-bedded conglomerate in Unit-3; (**D**), photograph of alternations of purplish-red medium- to thick-bedded medium- to fine-grained sandstone and medium- to thin-bedded silty mudstone in Unit-4, showing wedge-shaped pinch-outs in the sandstone beds; (**E**), photograph of alternations of purplish-red medium- to thick-bedded medium- to fine-grained sandstone and medium- to thin-bedded silty mudstone in Unit-4, showing typical large-scale trough cross-bedding in the sandstone beds; (**F**), climbing-ripple cross-lamination (F3) in the sandstone of Unit-4; (**G**), typical parallel bedding developed in the sandstone of Unit-4; (**H**), mud cracks in the silty mudstone of Unit-4; (**I**), burrows obliquely cutting across bedding planes in the sandstone of Unit-4.

Unit-4 comprises an irregular alternation of purplish-red, thick- to very thick-bedded, medium- to fine-grained sandstone and thin- to medium-bedded argillaceous siltstone and silty mudstone. The sandstone exhibits large-scale trough cross-bedding (F2; Figure 4E), locally contains climbing-ripple cross-lamination (F3; Figure 4F), and includes intervals of parallel bedding (F4; Figure 4G). Some sandstone beds have wedge-shaped geometries (Figure 4D). The argillaceous interbeds locally contain polygonal mud cracks (F6; Figure 4H), and trace fossils are preserved on oblique bedding planes (Figure 4I). The cross-bedded and parallel-bedded sandstone facies (F2 and F4) indicate current-driven sediment transport and deposition, whereas F3 records ripple migration accompanied by sediment accumulation [27,70,75,76]. The mud-rich facies F6 indicate intervals of reduced depositional energy and, where mud cracks are present, subsequent subaerial exposure [70,73]. The vertical alternation of sandy and fine-grained facies suggests repeated shifts between channel-related sedimentation and lower-energy deposition in adjacent overbank areas. The wedge-shaped sandstone geometries may reflect lateral variations in bed thickness or the geometry of individual sediment bodies, but do not, by themselves, provide sufficient evidence for lateral accretion. Unit-4 is therefore interpreted as a fluvial facies association comprising channel-related sandstone deposits and fine-grained overbank deposits. Such associations are consistent with fluvial systems in which channel migration and episodic overbank flooding influence sediment accumulation [27,70,75,76]. A meandering-river interpretation would be strengthened by evidence of lateral-accretion surfaces, systematic point-bar successions, and characteristic channel-body architecture. Because these diagnostic features are not explicitly documented in the available observations, the meandering-river interpretation remains provisional.

The dinosaur track-bearing surfaces provide additional evidence of local depositional conditions and the sequence of surface modification. On the DLW1 track-bearing surface, mud cracks intersect dinosaur footprints (Figure 2B), indicating that desiccation occurred after the footprints formed and subsequently modified them. This relationship suggests that the substrate was sufficiently moist and cohesive to preserve the footprints before subaerial exposure and drying. On the DLW2 track-bearing surface, straight, asymmetrical current ripples are preserved on the bedding surface (Figure 3A). Their approximately parallel crests indicate sediment transport by a predominantly unidirectional current. Dinosaur tracks superimposed on the ripple-marked surface indicate that ripple formation preceded footprint formation. Together, these structures record temporal variations in local flow conditions, substrate moisture, and subaerial exposure. They are consistent with a fluvial setting characterized by episodic inundation and exposure, but do not independently establish a specific channel or overbank subenvironment.

5.3. Paleogeographic Analysis of the Track Sites

Chinese reports of Middle Jurassic dinosaur tracks are abundant, with most track localities concentrated in Yunnan, Sichuan, and Shaanxi Provinces. Eastern Tibet has also yielded a wealth of research results in recent years (Figure 5; Appendix Table A1).

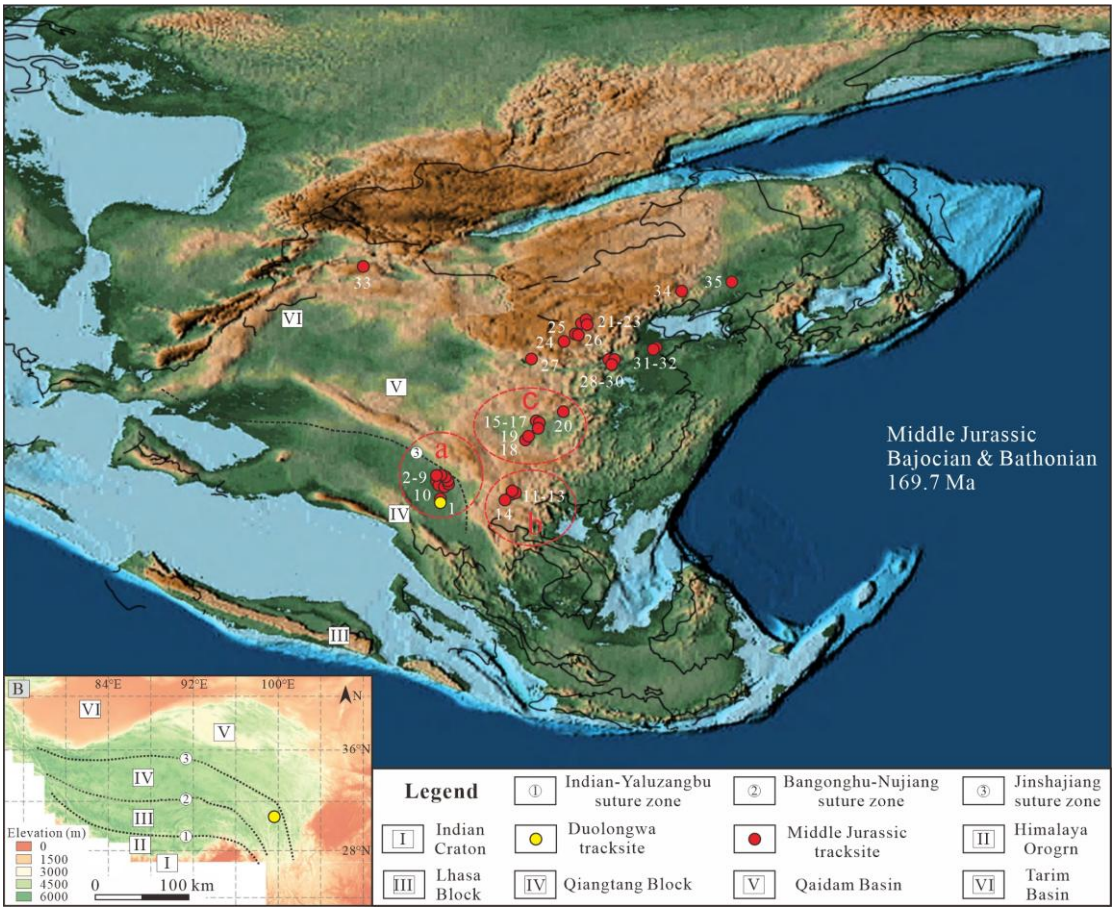


Figure 5. Paleogeographic map of East Asia during the Middle Jurassic, after Scotese [77], Chen [78], Ma and Hu [79], Wang et al. [80] and Li et al. [81]. Tracksite nos. 1–10 of the area a from the Changdu Basin, tracksite nos. 11–14 of the area b from the Yunnan Province, and tracksite nos. 15–20 of the area c from the Sichuan Province. (Tracksite numbers correspond to those in Appendix Table A1; Ma = million years showing the locations of Middle Jurassic tracksites.)

Sauropod track reports are relatively scarce for two reasons. First, dinosaur trackmaking [82]: sauropods were less active than theropods, resulting in fewer tracks. Second, we speculate that sauropod tracks are less rounded than the tridactyl tracks of theropods and ornithopods; therefore, they have attracted less attention. Among Middle Jurassic sauropod tracks from southwestern China, reports of *Brontopodus* mainly come from Lufeng [57] and Shuangbai [54] in Yunnan Province, as well as Karuo District, Changdu [17,22,26] and Chaya County [23] in eastern Tibet. The theropod track assemblage is broadly consistent with the global pattern. Li et al. [33] suggested that this theropod track assemblage can be assigned to the *Grallator–Anchisauripus–Eubrontes* plexus; *Kayentapus* is also a common ichnogenus. Among these, reports related to Middle Jurassic *Eubrontes* are the most abundant, with records from Karuo District, Changdu in eastern Tibet [27,28], Lufeng [57] and Shuangbai regions [58] in Yunnan Province, Zizhong County in Sichuan Province [83,84], and Zizhou County in Shaanxi [85].

Table 2. Lithofacies (F1–F6) of the Duolongwa Section.

Lithofacies	Diagnostic Lithology and Sedimentary Structures	Depositional Interpretation
F1: Massive sandstone facies	Medium- to fine-grained sandstone, commonly thick- to very thick-bedded, with no clearly discernible internal stratification at the outcrop scale	Sandy fluvial deposits; depositional position requires assessment of bed geometry and associated facies
F2: Cross-bedded sandstone facies	Medium- to fine-grained sandstone with trough cross-bedding	Current-driven sediment transport and deposition, commonly associated with fluvial channel processes
F3: Ripple-laminated sandstone facies	Sandstone with climbing-ripple cross-lamination; combined-flow ripple marks may occur on bedding surfaces	Ripple migration and sediment accumulation; associated combined-flow ripple marks indicate interaction between unidirectional currents and oscillatory flows
F4: Parallel-bedded sandstone facies	Sandstone displaying parallel bedding	Deposition under current-dominated conditions; the specific flow regime requires supporting sedimentological evidence
F5: Conglomeratic facies	Thin conglomerate beds with basal erosional scour surfaces; clasts are moderately to well sorted, subrounded to rounded, and preferentially oriented	Fluvial erosion and deposition of coarse-grained material, potentially representing channel-lag deposits
F6: Fine-grained mudstone and siltstone facies	Argillaceous siltstone and silty mudstone, locally poorly laminated and displaying polygonal mud cracks	Low-energy suspension deposition followed by intermittent subaerial exposure; potentially associated with overbank areas or floodplain depressions

The newly discovered sauropod tracks from the DLW2 sauropod tracklayer reported in this study are recently exposed tracks from the *Brontopodus* tracklayer reported by Xing et al. [23]. They suggest that these tracks are associated with the *Shunosaurus–Mamenchisaurus* fauna in the Sichuan and Yunnan provinces.

As for theropod tracks, Li et al. [25] proposed that the *Grallator anietangensis* trackmaker from eastern Tibet may have been related to *Shidaisaurus jinae*, a coeval theropod from the Sichuan Basin. In a subsequent study, Li et al. [27,33] suggested that the trackmaker of the *Eubrontes* tracks from eastern Tibet may have been related to *Gasosaurus constructus* from the Sichuan Basin.

Chen [86] was the first to propose that dinosaur faunas in southwestern China may have interacted, arguing that the Paleo-Dianzhong Lake in Yunnan and the Paleo-Bashu Lake in Sichuan provided hydrological conditions to facilitate interactions. Fang et al. [12] suggested that paleo-river systems such as the Paleo-Lancang River served as important corridors for dinosaur faunal exchange between Yunnan and eastern Tibet. Xing et al. [23] proposed that intermontane lowlands and tidal flats between the Sichuan Basin and the Qiangtang Block may have provided opportunities for the migration and exchange of dinosaur fauna. The newly discovered theropod and sauropod tracks from this study provide additional evidence for potential dinosaur faunal exchange between eastern Tibet and adjacent regions. However, it must be emphasized that track assemblage similarities can only serve as an important reference for reconstructing the paleogeographic distribution of dinosaur faunas. Similarities may also result from parallel evolution and do not necessarily indicate that the same trackmakers made the tracks. The theropod tracks from the Isle of Skye, Scotland, and the Duolongwa tracksite provide an opportunity to compare similarities in Jurassic theropod track morphology. Blakesley et al. [87] described a large theropod track, Morphotype 1a, from the Middle Jurassic Prince Charles's Point

tracksite on the Isle of Skye; it was subsequently assigned to Morphotype HBR_B1.1 [88]. Among the specimens assigned to HBR_B1.1, the convex-relief specimen SM.1976.2002.004 most closely resembles track 1-1-2 of Morphotype 1 from the Duolongwa tracksite, described in this study. Similarities include track size, the interdigital divarication angle between digits II and IV, the degree of mesaxony, and the morphology of the phalangeal pads. However, in the absence of associated dinosaur remains, it would be premature to conclude that the tracks were made by the same trackmaker. These discoveries nevertheless provide valuable material for comparative studies of Jurassic dinosaur track assemblages worldwide.

6. Conclusions

(1) The Duolongwa tracksite in the Middle Jurassic Dabuka Formation in Chaya County, Changdu Basin, eastern Tibet, comprises two tracklayers. DLW1 theropod tracklayer has twelve theropod tracks (Morphotype-1), which were assigned to Eubrontidae ichnogen. et ichnosp. indet. The DLW2 sauropod tracklayer has two sauropod tracks (Morphotype-2), which were likely made by *Brontopodus* isp. This finding provides new specimens for the Middle Jurassic dinosaur track assemblage in eastern Tibet.

(2) The trackmaker of Morphotype-1 had a hip height of 0.98–1.71 m and a body length of 2.59–4.48 m. The gaits of the T1 trackway's trackmaker and T2 trackway's trackmaker are both considered slow walking. Their movement speeds are 1.64 m/s and 2.18 m/s, respectively. Combined with coeval dinosaur remains from West China, *Gasosaurus constructus* is inferred as the most probable trackmaker of Morphotype-1. The trackmaker of Morphotype-2 possessed an estimated hip height of 2.96 m and a body length of 10.94 m. It was interpreted as a juvenile belonging to the *Shunosaurus–Mamenchisaurus* fauna.

(3) The paleoenvironment of the Duolongwa tracksite was a fluvial depositional system, consisting of channel and overbank subfacies. The substrate experienced intermittent subaerial exposure within this fluvial system, providing suitable conditions for the formation and preservation of dinosaur tracks. After track formation, the surfaces underwent subaerial desiccation, and mud cracks cut the tracks, indicating subaerial exposure within a fluvial setting.

(4) The Duolongwa tracksite suggests a close faunal connection between the Middle Jurassic dinosaur fauna of eastern Tibet and contemporaneous dinosaur faunas in the Sichuan and Yunnan provinces, supporting the existence of migration corridors for dinosaur dispersal between these regions. However, because similarities in ichnomorphology cannot rule out parallel evolution, more dinosaur remains are needed to substantiate exchange and interaction among Jurassic dinosaur faunas in southwest China.

Author Contributions: Writing—original draft preparation, G.Z.; conceptualization, G.Z. and L.Y. (Li Yangui); methodology, L.Y. (Li Yangui) and X.L.; validation, L.Y. (Li Yangui), Y.H., X.L. and C.L.; investigation, L.Y. (Liu Yilei), W.J. and Y.Q.; resources, L.Y. (Li Yangui), Y.H. and Y.Q.; data curation, Y.Q. and H.J. All authors have read and agreed to the published version of the manuscript.

Funding: This research was supported by the Bijie City Joint Science and Technology Fund Project (Nos. Bi Ke Lian He No. [2025]1, [2025]2 and 2023BKH56), the National Natural Science Foundation of China (No. 42530205), the Guizhou Science and Technology Support Project (No. [2023] 131), the Key Laboratory of Critical Mineral Resources Exploration and Development of Bijie City (No. Bi Ke He [2024] No. 21), the Fund of Department of Natural Resources of Tibet Autonomous Region (No. 5400002321020001), and the Natural Scientific Research Project of the Guizhou Provincial Department of Education (Nos. QJHKYZ [2015]340, QJJ [2022]124, QJJ [2024]012).

Data Availability Statement: Data are contained within the article.

Acknowledgments: The fieldwork for this study received strong support and assistance from the Tibet Autonomous Region Department of Natural Resources, the Tibet Autonomous Region Bureau of Geological and Mineral Exploration and Development, the Changdu Municipal Bureau of Natural Resources, and the Chaya County Bureau of Natural Resources. Thanks go to the editors and the reviewers for their constructive comments and suggestions on the revision of the paper.

Conflicts of Interest: The authors declare no conflict of interest.

Appendix A

Table A1. Middle Jurassic ichnotaxa form China, eastern Asia.

Nos.	Place	Location	Formation	Type	Ichnotaxon	References
1	Changdu, Tibet	Chaya County	Dabuka Fm.	Theropod	Eubrontidae igen. et isp. indet.	This study
				Sauropod	*Brontopodus* isp.	
2	Changdu, Tibet	Karuo District	Dabuka Fm.	Theropod	*Eubrontes* isp.	Li et al. [27]
					—	
					—	
3	Changdu, Tibet	Karuo District	Dabuka Fm.	Theropod	*Grallator anietangensis*	Li et al. [25]
					—	
4	Changdu, Tibet	Karuo District	Dabuka Fm.	Theropod	*Weidichnus* isp.	Li et al. [26]
				Sauropod	*Brontopodus*	
5	Changdu, Tibet	Karuo District	Dabuka Fm.	Sauropod	*Brontopodus*	Yao et al. [24]
				Ornithopod	—	
6	Changdu, Tibet	Karuo District	Dabuka Fm.	Theropod	—	Weise et al. [29]
7	Changdu, Tibet	Karuo District	Chaya Gr.	Sauropod	*Brontopodus*	Xing et al. [22]
8	Changdu, Tibet	Karuo District	Chaya Gr.	Sauropod	*Brontopodus*	Xing et al. [17]
9	Changdu, Tibet	Karuo District	Dongdaqiao Fm.	Theropod	Eubrontidae	Chen et al. [28]
				Sauropod	cf. *Parabrontopodus* isp.	
10	Changdu, Tibet	Chaya County	Dongdaqiao Fm.	Stegosaurus	*Deltapodus* isp.	Xing et al. [23]
				Sauropod	cf. *Brontopodus*	
11	Lufeng, Yunnan	Konglongshan Town	Chuanjie Fm.	Theropod	*Lufengopus*	Lü et al. [52]
12	Lufeng, Yunnan	Konglongshan Town	Chuanjie Fm.	Theropod	*Eubrontes*	Xing et al. [57]
				Sauropod	*Brontopodus*	
13	Lufeng, Yunnan	Konglongshan Town	Chuanjie Fm.	Stegosaurus	cf. *Stegopodus*	Xing et al. [89]
14	Shuangbai, Yunnan	Hemenkou	Shedian Fm. (J_{2-3})	Theropod	—	Xing et al. [58]
					Grallator	
				Theropod	Eubrontidae	
				Sauropod	*Brontopodus*	
15	Zizhong, Sichuan	Wuhuang Town	Xintiangou Fm.	Theropod	*Eubrontes* isp.	Yang and Yang [83]
16	Zizhong, Sichuan	Wuhuang Town	Xintiangou Fm.	Theropod	*Chuanchengpus shenglingshanensis*	Lockley et al. [84]
					Gigandipus hei	
					Eubrontes nianpanshanensis	
					Grallator wuhuangensis	

					Kayentapus jizhuashiensis *Grallator microiscus*	
17	Zigong, Sichuan		J_2	Theropod	*Gigandipus*	Xing et al. [61]
18	Huidong, Sichuan	Huidong Town	Xincun Fm.	Theropod	cf. *Kayentapus*	Xing et al. [90]
19	Meigu, Sichuan	Bingtu Town	Shaximiao Fm.	Theropod	*Carmelopodus*	Xing et al. [91]
20	Xuanhan, Sichuan	Qili Town	Xintiangou Fm.	Ornithopod	cf. *Anomoepus*	Xing et al. [92]
21	Shenmu, Shaanxi	Langanbao Town	Yanan Fm.	Theropod	*Grallator*	Li et al. [93]
22	Shenmu, Shaanxi	Langanbao Town	Yanan Fm.	Stegosaurus	*Shenmuichnus youngteilhardi*	Li et al. [94]
23	Shenmu, Shaanxi	Langanbao Town	Yanan Fm.	Ornithopod	*Anomoepus*	Li et al. [93]
24	Tongchuan, Shaanxi	Jiaopingmeikuang	Zhiluo Gr.	Theropod	*Shensipus tunchuanensis*	Young [95]
25	Zizhou, Shaanxi	Dianshi Town	Yanan Fm.	Theropod	*Eubrontes* *Kayentapus* *Anomoepus* *Deltapodus* isp.	Xing et al. [85]
26	Zizhou, Shaanxi	Dianqi Town	Yanan Fm.	Theropod	*Zizhpupus wangi* *Changpeipus longweimaoensis* *Shensipus xiaoliheensis* *Shensipus tunchuanensis*	Li and Zhang [96]
27	Baiying, Gansu	Baoji Town	Wangjiashan Fm.	Theropod	*Grallator pingchuanensis*	Li et al. [97]
28	Yima, Henan	Yima City	Yima Fm.	Theropod	*Kayentapus* isp.	Li et al. [93]
29	Yima, Henan	Yima City	Yima Fm.	Theropod	*Changpeipus xuiana*	Lü et al. [98]
30	Yima, Henan	Yima City	Yima Fm.	Ornithopod	*Anomoepus*	Xing et al. [99]
31	Xintai, Shandong	Runan Town	Santai Fm.	Theropod	cf. *Grallator*	Li et al. [100]
32	Xintai, Shandong	Runan Town	Santai Fm.	Theropod	cf. *Velociraptorichnus*	Li et al. [93]
33	Shanshan, Xinjiang	Qiketai Town	Sanjianfang Fm.	Theropod	*Changpeipus carbonicus*	Xing et al. [99]
34	Beipiao, Liaoning	Nanbajiazi Town	Tuchengzi Fm. (J_{2-3})	Theropod	*Grallator*	Li et al. [93]
35	Huinan, Jilin	Songshangang	J_{1-2}	Theropod	*Changpeipus*	Young [48]; Li [101]

Note: Fm. = Formation; Gr. = Group; J_{2-3} = Middle and Upper Jurassic; J_2 = Middle Jurassic; J_{1-2} = Lower and Middle Jurassic.

References

1. Mao, L.; Xing, L.D.; Zhang, J.P.; Wang, T.; Wang, D. Revisiting the world-famous Lufeng Formation dinosaur fauna: New approaches to old problems. *Hist. Biol. Int. J. Paleobiol.* **2019**, *32*, 1–9.
2. Li, K. The fossil sauropods of China and their stratigraphic horizons. *J. Chengdu Univ. Technol.* **1998**, *25*, 54–60.
3. Sekiya, T. *A New Study of the Sauropod Dinosaur Anachuanlong from the Middle Jurassic Chuanjie Formation of Lufeng, Yunnan, China*; Jilin University: Jilin, China, 2010.
4. Peng, G.Z. Assemblage characteristics of the Jurassic dinosaur fauna from Zigong, Sichuan, China. *Geol. J. China Univ.* **2009**, *33*, 113–123.
5. Ye, Y.; Peng, G.Z.; Jiang, S. Preliminary study on the histology of long bones of Shunosaurus and Omeisaurus from the Middle Jurassic Dashanpu fauna, Zigong, Sichuan, China. *Acta Palaeontol. Sin.* **2007**, *46*, 135–144.
6. Ouyang, H. *Skeletal Features of Mamenchisaurus Youngi and the Phylogenetic Relationships of Mamenchisaurid Dinosaurs*; Chengdu University of Technology: Chengdu, UK, 2003.

7. Yang, C.Y. *Phylogeny of Mamenchisauridae*; Chengdu University of Technology: Chengdu, China, 2014.
8. Hu, H.Q. *Taphonomy of Dinosaur Footprints and Skeletal Fossils from the Lower Jurassic Lufeng Formation, Yunnan, China*; China University of Geosciences: Beijing, China, 2016.
9. Wang, J.; Ye, Y.; Pei, R.; Tian, Y.; Feng, C.; Zheng, D.; Chang, S.-C. Age of Jurassic basal sauropods in Sichuan, China: A reappraisal of basal sauropod evolution. *Geol. Soc. Am.* **2018**, *130*, 1493–1500.
10. Xia, D.X.; Liu, S.K.; Teng, Y.; Zhang, J.M.; Xu, K.F.; Xie, Y.M.; Yao, Z.F.; Wu, T.Y.; Xiao, X.M. *Stratigraphy of the Tibet Autonomous Region*; China University of Geosciences Press: Wuhan, China, 1997.
11. Sun, C.R.; Chen, G.L.; Li, Z.R.; La, J.D.; Liu, G.C.; Ji, L.X.; Sun, J.B.; Wang, D.Q. *Stratigraphy of Qinghai Province*; China University of Geosciences Press: Wuhan, China, 1997.
12. Fang, X.S.; Zhang, Z.J.; Lu, L.W.; Han, Y.J.; Zhao, X.J.; Li, P.X. Collision between the Indian Plate and the Paleo-Asian Plate and the emergence of Asian dinosaurs. *Geol. Bull. China* **2006**, *25*, 862–873.
13. Chao, X.J. First discovery of dinosaur fossils in Tibet. *Stratigr. Palaeontol. Commun.* **1978**, *9*, 112–114.
14. Chao, X.J. The reptilian fauna of the Jurassic. In *Stratigraphy of China 11: Jurassic of China*; Wang, S.E., Cheng, Z.W., Wang, N.W., Liu, S.W., Xu, F.X., Zhang, W.P., Zhang, Z.C., Yu, Q.S., Dong, G.Y., Yao, J.X., Sun D.L., et al., Eds.; Geological Publishing House: Beijing, China, 1985.
15. An, X.Y.; Wang, Q.Y.; Li, Y.; Wang, B.D.; Wang, D.B. New discovery of Jurassic dinosaur fossils in Chaya area, Qamdo, Tibet. *Geol. Bull. China* **2021**, *40*, 189–193.
16. Wei, X.F.; Wang, Q.Y.; An, X.Y.; Wang, B.D.; Zhang, Y.J.; Mou, C.L.; Li, Y.; Wang, D.B.; Ma, W.; Kundrát, M. New sauropod remains from the Middle Jurassic Dongdaqiao Formation of Qamdo, eastern Tibet. *Palaeoworld* **2024**, *33*, 744–752.
17. Xing, L.D.; Harris, J.D.; Philip, J.C. First record of a dinosaur trackway from Tibet, China. *Geol. Bull. China* **2011**, *30*, 173–178.
18. Chao, X.J. Phylogeny and evolutionary stages of Dinosauria. *Acta Palaeontol. Pol.* **1983**, *28*, 295–306.
19. Dong, Z.M.; You, H.L.; Peng, G.Z. *China Vertebrate Fossils: Vol. 2. Amphibians, Reptiles, Birds. Fascicle 5. Ornithischian dinosaurs*; Science Press: Beijing, China, 2015.
20. Dong, Z.M. Stegosaurus of Asia. In *Dinosaur Systematics and Approaches*; Carpenter, K., Currie, P.J., Eds.; Cambridge University Press: Cambridge, UK, 1990; pp. 255–268.
21. Maidment, S.C.R.; Wei, G.B. A review of the Late Jurassic stegosaurs (Dinosauria, Stegosauria) from the People's Republic of China. *Geol. Mag.* **2006**, *143*, 621–634.
22. Xing, L.D.; Xu, X.; Lockley, M.G.; Klein, H.; Zhang, L.J.; Persons, W.S.; Wang, D.H.; Wang, M.Y.; Wan, X.Q. Sauropod trackways from the Middle Jurassic Chaya Group of eastern Tibet, China. *Hist. Biol. Int. J. Paleobiol.* **2021**, *33*, 3141–3151.
23. Xing, L.; Klein, H.; Lockley, M.G.; Li, H.; Tong, B.; Ye, Y.; Dai, H.; Chunyong, C.; Wang, D.; Romilio, A.; Persons, W.S. New records of dinosaur tracks in eastern Tibet and a review of Middle Jurassic dinosaur faunas from the eastern Tethys, southwest China. *Hist. Biol. Int. J. Paleobiol.* **2024**, *36*, 1244–1258.
24. Yao, H.Z.; Li, Y.G.; Junaid, K.; Asma, T.; An, Z.H.; Zhao, H.; Zhang, L.; Lyu, Z.Y.; Wang, X.D.; Zhao, L.S.; Wang, J.X.; He, Y.Y.; An, X.Y.; Zhang, R.J. Discovery of rare dinosaur track assemblages and paleelephant track assemblages in eastern Tibet. *J. Cent. China Norm. Univ. (Nat. Sci.)* **2021**, *55*, 919–924.
25. Li, Y.G.; Yao, H.Z.; William, J.F.; Xing, L.D.; Wang, C.S.; Asma, T.; Junaid, K.; An, Z.H.; Zhao, H.; Wang, J.X. First discovery of Middle Jurassic theropod dinosaur tracks in Qamdo, eastern Tibet. *Earth Sci.* **2022**, *47*, 4223–4245.
26. Li, Y.G.; Yao, H.Z.; Asma, T.; Junaid, K.; William, J.F.; Wang, P.; Zhao, L.S.; An, Z.H.; Wang, C.S.; Wang, J.X. Discovery of Middle Jurassic small theropod footprints in eastern Tibet, China. *J. Earth Sci.* **2024**, *35*, 1820–1831.
27. Li, Y.G.; Zhao, H.; William, J.F.; Yu, Y.; Cai, Q.S.; An, Z.H.; Wang, C.S.; Sang, Y.H.; Yao, H.Z. Middle Jurassic theropod tracks from the Wenda tracksite, eastern Xizang, China. *J. Earth Sci.* **2026**, *37*, 1036–1054.
28. Chen, X.Y.; Xing, L.D.; Zhang, H.C.; Chen, Q.Y.; Yang, J.Y.; Jin, Y.F.; Zhu, N.; Teng, C. Newly discovered tracksites from the Middle Jurassic Chaya Group of eastern Tibet, China, with implications for saurischian distribution around the eastern Tethys. *Hist. Biol. Int. J. Paleobiol.* **2025**, *37*, 2318–2327.
29. Weise, J.C.; Gesang, C.R.; Lü, D.K.; Ye, Q.; Bao, F.R.; Suolang, D.Z.; Zhang, Z.; Tan, H.P.; Bianba, C.R. New discoveries of dinosaur fossils and geological heritage in eastern Tibet. *Tibet. Sci.* **2024**, *46*, 45–51.
30. Li, Y.G.; Zhao, H.; William, J.F.; Yu, Y.; Xing, L.D.; Ye, Q.; Wang, C.S.; Yao, H.Z. First discovery of dinosaur tracks from the Lower Cretaceous Duoni Formation in eastern Tibet, China. *Cretac. Res.* **2025**, *166*, 106009.
31. Li, Y.G.; Yao, H.Z.; Yue, Y.; Foster, W.J.; Wang, C.S.; Zhao, L.S.; Xing, L.D. First report of sauropod and ornithopod tracks from the Upper Cretaceous of Tibet, China. *Cretac. Res.* **2023**, *149*, 105569.

32. Xing, L.D.; Chou, C.Y.; Lockley, M.G.; Yangchen, D.; Chen, X.R.; Ma, X.H.; Zhou, W.J.; Xu, H.T. First report of avian tracks from the Cretaceous of Tibet, China. *Acta Geol. Sin.* **2017**, *91*, 2312–2313.
33. Li, Y.G. *Study on Jurassic Dinosaur Footprints in Qamdo, Eastern Tibet*; China University of Geosciences: Wuhan, China, 2024.
34. Wang, L.Q.; Pan, G.T.; Ding, J. *Geological Map of the Qinghai-Tibet Plateau and Adjacent Areas (1:1,500,000)*; Geological Publishing House: Beijing, China, 2013.
35. He, J.H. *Stratigraphic Framework and Sedimentary Basin Evolution of the Jurassic Rocks in the Lancang River Region of Eastern Tibet*; Chengdu University of Technology: Chengdu, China, 2018.
36. Song, L.B.; Cong, S.; Zhang, Y.; Wan, C.B.; Pei, J.B.; Zhang, M.S. Palynological assemblage characteristics and geological significance of the Denglouku Formation in the Fushuangda area, southern Songliao Basin. *Unconv. Oil Gas* **2025**, *12*, 11–24.
37. Zhen, S.N.; Li, J.J.; Han, Z.K.; Yang, X.L. *The Study of Dinosaur Footprints in China*; Sichuan Scientific and Technological Publishing House: Chengdu, China, 1996.
38. Thulborn, T. *Dinosaur Tracks*; Chapman and Hall: London, UK, 1990.
39. Olsen, P.E.; Smith, J.B.; McDonald, N.G. Type material of the type species of the classic theropod footprint genera Eubrontes, Anchisauripus, and Grallator (Early Jurassic, Hartford and Deerfield basins, Connecticut and Massachusetts, U.S.A.). *J. Vertebr. Paleontol.* **1998**, *18*, 586–601.
40. Lockley, M.G. New perspectives on morphological variation in tridactyl footprints: Clues to widespread convergence in developmental dynamics. *Geol. Q.* **2009**, *53*, 415–432.
41. Xing, L.; Lockley, M.G.; Klein, H.; Falkingham, P.L.; Kim, J.Y.; Mccrea, R.T.; Zhang, J.; Persons, W.S.; Wang, T.; Wang, Z. First Early Jurassic small ornithischian tracks from Yunnan Province, southwestern China. *Palaios* **2016**, *31*, 516–524.
42. Henderson, D.M. Footprints, trackways and hip heights of bipedal dinosaurs: Testing hip height predictions with computer models. *Ichnos Int. J. Plant Anim. Traces* **2003**, *10*, 99–144.
43. Alexander, R.M. Estimates of speeds of dinosaurs. *Nature* **1976**, *261*, 129–130.
44. Farlow, J.O. Sauropod tracks and trackmakers: Integrating the ichnological and skeletal record. *Zubia* **1992**, *10*, 89–138.
45. Li, R.; Lockley, M.G.; Matsukawa, M.; Wang, K.; Liu, M. An unusual theropod track assemblage from the Cretaceous of the Zhucheng area, Shandong Province, China. *Cretac. Res.* **2011**, *32*, 422–432.
46. Lull, R.S. *Triassic life of the Connecticut Valley*; Connecticut Geological and Natural History Survey, Bulletin; State Geological and Natural History Survey: Madison, WI, USA, 1953; Volume 81, pp. 1–334.
47. Matsukawa, M.; Shibata, K.; Kukihara, R.; Koarai, K.; Lockley, M.G. Review of Japanese dinosaur track localities: Implications for ichnotaxonomy, paleogeography and stratigraphic correlation. *Ichnos Int. J. Plant Anim. Traces* **2005**, *12*, 201–222.
48. Young, C.C. Fossil footprints in China. *Vertebr. Palasiat.* **1960**, *4*, 53–67.
49. Li, J.J.; Bartel; Zhang, W.H.; Hu, B.L.; Gao, L.H. Fossil giant sauropod footprints from the Chabu area, Inner Mongolia, China. *Acta Palaeontol. Sin.* **2006**, *45*, 221–234.
50. Hitchcock, E. An attempt to name, classify, and describe the animals that made the fossil footmarks of New England. In Proceedings of the 6th Annual Meeting of the Association of American Geologists and Naturalists, New Haven, CT, USA, April 1845; Volume 6, pp. 23–25.
51. Zeng, X.Y. Dinosaur footprint fossils discovered in the red beds of the Yuanma Basin, northwestern Hunan, China. *Hunan Geol.* **1982**, *1*, 57–58+104.
52. Lü, J.C.; Azuma, Y.; Wang, T.; Li, S.X.; Pan, S.G. The first discovery of dinosaur footprints from Lufeng, Yunnan Province, China. *Mem. Fukui Prefect. Dinosaur. Mus.* **2006**, *5*, 35–39.
53. Li, J.J.; Bai, Z.Q.; Wei, Q.Y. *Dinosaur tracks from the Upper Cretaceous of Etuoke Banner, Inner Mongolia, China*; Geological Publishing House: Beijing, China, 2011.
54. Xing, L.D.; Lockley, M.G.; Zhang, J.P.; Klein, H.; Li, D.Q.; Miyashita, T.; Li, Z.D.; Kümmell, S.B. A new sauropodomorph ichnogenus from the Lower Jurassic of Sichuan, China fills a gap in the track record. *Hist. Biol. Int. J. Paleobiol.* **2016**, *28*, 881–895.
55. Lockley, M.G.; Farlow, J.O.; Meyer, C.A. Brontopodus and Parabrontopodus ichnogen. nov. and the significance of wide and narrow-gauge sauropod trackways. *Gaia* **1994**, *10*, 135–146.
56. Farlow, J.O.; Pittman, J.G.; Hawthorne, J.M. Brontopodus birdi, Lower Cretaceous dinosaur footprints from the U.S. Gulf Coast Plain. In *Dinosaur Tracks and Traces*; Gillette, D.D., Lockley, M.G, Eds.; Cambridge University Press: Cambridge, UK, 1989.
57. Xing, L.-D.; Lockley, M.G.; Miyashita, T.; Klein, H.; Wang, T.; Persons, W.S.; Pan, S.-G.; Zhang, J.-P.; Dong, Z.-M. Large sauropod and theropod tracks from the Middle Jurassic Chuanjie Formation of Lufeng County, Yunnan Province, and palaeobiogeography of the Middle Jurassic sauropod tracks from southwestern China. *Palaeoworld* **2014**, *23*, 294–303.

58. Xing, L.-D.; Lockley, M.G.; Zhang, J.-P.; Klein, H.; Wang, T.; Kümmell, S.B.; Burns, M.E. A theropod-sauropod track assemblage from the ?Middle-Upper Jurassic Shedian Formation at Shuangbai, Yunnan Province, China, reflecting different sizes of trackmakers: Review and new observations. *Palaeoworld* **2016**, *25*, 84–94.
59. Abrahams, M.; Bordy, E.M.; Knoll, F. Hidden for one hundred years: A diverse theropod ichnoassemblage and cross-sectional tracks from the historic Early Jurassic Tsikoane ichnosite (Clarens Formation, northern Lesotho, southern Africa). *Hist. Biol. Int. J. Paleobiol.* **2021**, *33*, 2504–2519.
60. Farlow, J.O. *Noah's Ravens: Interpreting the Makers of Tridactyl Dinosaur Footprints*; Indiana University Press: Indiana, IN, USA, 2018.
61. Xing, L.D.; Peng, G.Z.; Ye, Y.; Klein, H.; Lockley, M.G.; Wang, T.; Persons, W.S. Large theropod trackway from the Lower Jurassic Zhenzhuchong Formation of Weiyuan County, Sichuan Province, China: Review, new observations and special preservation. *Palaeoworld* **2014**, *23*, 284–294.
62. Rauhut, O.W.M. The interrelationships and evolution of basal theropod dinosaurs. *Spec. Pap. Palaeontol.* **2003**, *69*, 1–213.
63. Dong, Z.M.; Tang, Z.L. A new Mid-Jurassic theropod (Gasosaurus constructus gen. et sp. nov.) from Dashanpu, Zigong, Sichuan Province, China. *Vertebr. Palasiat.* **1985**, *23*, 77–83+99–100.
64. Zhang, Y.H. *Shu Dinosaur from the Middle Jurassic Dinosaur Fauna of Dashanpu, Zigong, Sichuan, China (Volume III: Sauropods I)*; Sichuan Science and Technology Press: Chengdu, China, 1988.
65. He, X.L.; Li, K.; Cai, K.J. *Tianfu Omeisaurus from the Middle Jurassic Dinosaur fauna of Dashanpu, Zigong, Sichuan, China (Volume IV: Sauropods II)*; Sichuan Science and Technology Press: Chengdu, China, 1988.
66. Zhang, Y.H.; Li, K.; Zeng, Q.H. A new sauropod species from the Late Jurassic of the Sichuan Basin. *J. Chengdu Univ. Technol.* **1998**, *25*, 61–70.
67. An, X.Y.; Xu, X.; Han, F.L.; Wang, Q.Y.; Wang, B.D.; Wang, D.B. A new juvenile sauropod specimen from the Middle Jurassic Dongdaqiao Formation of East Tibet. *PeerJ* **2023**, *11*, e14982.
68. Zhang, Y.H.; Yang, D.H.; Peng, G.Z. New materials of Shu Dinosaur from Dashanpu, Zigong, Sichuan, China. *J. Chengdu Inst. Geol.* **1984**, *11*, 1–12.
69. Peng, G.Z.; Ye, Y.; Gao, Y.H.; Shu, C.K.; Jiang, S. *Jurassic Dinosaur Fauna of Zigong Region*; Sichuan People's Publishing House: Chengdu, China, 2005.
70. Chen, J.Q.; Zhou, H.R.; Wang, X.L. Sedimentology and Paleogeography. Beijing: Geological Publishing House, 2019.
71. Collinson, J.D.; Thompson, D.B. *Sedimentary Structures*, 3rd ed.; Dunedin Academic Press: Harpenden, UK, 2006.
72. Bian, M.; Zhu, B.H.; Tan, Y.Y.; Shi, F.P.; Zhang, S.D.; Yang, Y.L.; Sun, X.Q. Sedimentary characteristics and genetic model of tidal sand bars in the western slope of the Xihu Sag, East China Sea Shelf Basin: A case study of the middle-upper Eocene Pinghu Formation in the inner belt of the Pinghu slope. *Unconv. Oil Gas* **2026**, *13*, 40–49.
73. Li, C. Sedimentary characteristics of a low-sinuosity meandering river in the lower Member of the Mingxi section, Laibei low uplift, Bohai Bay Basin. *Unconv. Oil Gas* **2024**, *11*, 22–28.
74. Zhi, L.F.; Wang, Y.K.; Liu, J.X.; Zhang, Y.Q. Reservoir architecture research based on production dynamic verification: A case study of the He 8 reservoir in the Yan X well area of the Yan'an gas field. *Unconv. Oil Gas* **2026**, *13*, 104–119.
75. Du, Y.S.; Yang, J.H.; Yu, W.C.; Yang, W.T. *Fundamentals of Sedimentary Geology*; China University of Geosciences Press: Wuhan, China, 2022.
76. Li, J.X.; Liu, E.H.; Hu, L.L.; Zhang, Y.L.; Li, J.; Zhang, Q.; Wu, X.B.; Liu, M.M. Reservoir characteristics of Member Shan 1 in the western area of the Yan'an gas field, Ordos Basin, and their control on gas reservoirs. *Unconv. Oil Gas* **2025**, *12*, 35–44.
77. Scotese, C.R. Map Folio 37 Middle Jurassic (Bajocian & Bathonian, 169.7 Ma). Available online: https://www.researchgate.net/publication/272944213_Map_Folio_37_Middle_Jurassic_Bajocian_Bathonian_1697_Ma (accessed on 1 December 2013).
78. Chen, Y.F. *Subduction-Collision Process in the Eastern Segment of Bangong Nujiang Suture Zone*; University of Chinese Academy of Sciences: Beijing, China, 2020; pp. 1–296, 4 pls. (In Chinese)
79. Ma, A.L.; Hu, X.M. Constraining the obduction process of the Dongqiao ophiolite in the Bangongco-Nujiang suture zone by the sedimentary record . *Sediment. Geol. Tethyan Geol.* **2021**, *41*, 163–175.
80. Wang, Y.J.; Lu, X.H.; Qian, X.; Wu, S.N.; Zhang, Y.Z.; Wang, Y. Prototethyan orogenesis in southwest Yunnan and Southeast Asia. *Sci. China Earth Sci.* **2022**, *65*, 1921–1947.
81. Li, Y.G.; Huang, Y.G.; Fan, C.C.; William, J.F.; Cai, Q.S.; Xing, L.D.; Ye, Q.; Fang, Z.C.; Yao, H.Z. Dinosaur track assemblages from the Middle Jurassic of eastern Tibet, China: Insights into dinosaur diversity, paleoenvironment and paleobiogeography. *J. Earth Sci.* **2026**. Available online: https://link.cnki.net/urlid/42.1788.P.20260805.0939.004 (accessed on 5 August 2026).

82. Farlow, J.O. *Lower Cretaceous Dinosaur Tracks, Paluxy River Valley, Texas*; GSA South-Central Section, Baylor University: Waco, TX, USA, 1987; pp. 1–50.
83. Yang, X.L.; Yang, D.H. *Dinosaur Footprints of the Sichuan Basin*; Sichuan Science and Technology Press: Chengdu, China, 1987.
84. Lockley, M.G.; Li, J.J.; Li, R.H.; Matsukawa, M.; Harris, J.D.; Xing, L.D. A review of the theropod track record in China, with special reference to type ichnospecies: Implications for ichnotaxonomy and paleobiology. *Acta Geol. Sin.* **2013**, *87*, 1–20.
85. Xing, L.D.; Lockley, M.G.; Tang, Y.G.; Klein, H.; Zhang, J.P.; Persons, W.S.; Dai, H.; Ye, Y. Theropod and ornithischian footprints from the Middle Jurassic Yanan Formation of Zizhou County, China. *Ichnos Int. J. Plant Anim. Traces* **2015**, *22*, 1–11.
86. Chen, P.J. Jurassic and Cretaceous paleogeographic outline of China: With a discussion on the origin of the Yangtze River. *Peking Univ. J. (Nat. Sci. Ed.)* **1979**, *3*, 90–109.
87. Blakesley, T.; dePolo, P.E.; Wade, T.J.; Ross, D.A.; Brusatte, S.L. A new Middle Jurassic lagoon margin assemblage of theropod and sauropod dinosaur trackways from the Isle of Skye, Scotland. *PLoS ONE* **2025**, *20*, e0319862.
88. Blakesley, T.; dePolo, P.E.; Ross, D.A.; Clark, N.D.L.; Brusatte, S.L. Small theropod-dominated dinosaur footprint assemblages in the Middle Jurassic Valtos Sandstone and Kilmaluag Formations on the Isle of Skye, Scotland. *R. Soc. Open Sci.* **2025**, *12*, 251016.
89. Xing, L.D.; Lockley, M.G.; Klein, H.; Ye, Y.; Zhang, J.P.; Wang, T.; Persons, W.S. First thyreophoran type tracks from the Middle Jurassic Chuanjie Formation of Yunnan Province, China. *Ichnos Int. J. Plant Anim. Traces* **2019**, *26*, 8–15.
90. Xing, L.D.; Lockley, M.G.; Li, Z.D.; Klein, H.; Zhang, J.P.; Wang, T.; Persons, W.S. Middle Jurassic theropod trackways from the Panxi region, Southwest China and a consideration of their geologic age. *Palaeoworld* **2013**, *22*, 36–41.
91. Xing, L.D.; Ba, J.; Lockley, M.G.; Klein, H.; Zhang, J.P.; Wang, T.; Persons, W.S. Late Triassic sauropodomorph and Middle Jurassic theropod tracks from the Xichang Basin, Sichuan Province, southwestern China: First report of the ichnogenus Carmelopodus. *Biopalaeogeography Palaeoecol.* **2018**, *7*, 1–13.
92. Xing, L.D.; Lockley, M.G.; Wang, Y.D.; Pole, M.S.; Klein, H.; Peng, G.Z.; Xie, X.P.; Zhang, G.Q.; Deng, C.T.; Burns, M.E. New Middle Jurassic dinosaur track record from northeastern Sichuan Province, China. *Swiss J. Palaeontol.* **2017**, *136*, 359–364.
93. Li, R.H.; Li, J.J.; Xing, L.D. *Atlas of Dinosaur Tracks from China*; Qingdao Publishing House: Qingdao, China, 2021.
94. Li, J.J.; Lockley, M.J.; Zhang, Y.G.; Xing, L.D.; Wang, T.; Ye, Y.; Klein, H. An important ornithischian tracksite in the Early Jurassic of the Shenmu Region, China. *Acta Geol. Sin.* **2012**, *86*, 1–10.
95. Young, C.C. Two footprints from the Jiaoping Coal Mine of Tungchuan, Shensi. *Vertebr. Palasiat.* **1966**, *10*, 68–71.
96. Li, Y.X.; Zhang, Y.X. Early Middle Jurassic dinosaur footprints from Zizhou County, China. *Vertebr. Palasiat.* **2017**, *55*, 276–288.
97. Li, D.Q.; Xing, L.D.; Lockley, M.G.; Klein, H.; Zhang, J.P.; Wang, T.; Persons, W.S. The first theropod tracks from the Middle Jurassic of Gansu, Northwest China: New and rare evidence of quadrupedal progression in theropod dinosaurs. *J. Palaeogeogr.* **2019**, *8*, 198–208.
98. Lü, J.C.; Zhang, X.L.; Jia, S.H.; Wang, T.; Dong, Z.M. The discovery of theropod dinosaur footprints from the Middle Jurassic Yima Formation of Yima County, Henan Province. *Acta Geol. Sin.* **2007**, *81*, 439–445.
99. Xing, L.D.; Klein, H.; Lockley, M.G.; Ye, Y.; Zhang, J.P.; Wang, T.; Persons, W.S. *Changpeipus* (theropod) tracks from the Middle Jurassic of the Turpan Basin, Xinjiang, Northwest China: Review, new discoveries, ichnotaxonomy, preservation and paleoecology. *Vertebr. Palasiat.* **2014**, *52*, 1–14.
100. Li, R.H.; Liu, M.W.; Du, S.X. Dinosaur tracks from Middle-Upper Jurassic Santai Formation: New materials and new interpretation. *Shandong Land Resour.* **2015**, *31*, 1–3.
101. Li, J.J. *Palaeovertebrata Sinica. Amphibians, Reptilians, and Avians. Footprints of Mesozoic Reptilians and Avians*; Science Press: Beijing, China, 2015.

Disclaimer/Publisher's Note: The statements, opinions and data contained in all publications are solely those of the individual author(s) and contributor(s) and not of MDPI and/or the editor(s). MDPI and/or the editor(s) disclaim responsibility for any injury to people or property resulting from any ideas, methods, instructions or products referred to in the content.